



Full Length Article

Evaluation of Photosynthetic Characters and Regulation Pattern of Photosynthesis Associated Gene in Two Mulberry Varieties

Yong Li^{1,2}, Cui Yu², Rongli Mo², Chao Xiong², Zhixian Zhu², Xingming Hu², Chuxiong Zhuang^{1*} and Wen Deng^{2*}

¹College of Life Sciences, South China Agricultural University, Guangzhou 510642, China

²Cash Crops Research Institute, Hubei Academy of Agricultural Sciences, Wuhan 430064, China

*Corresponding authors: 68568911@qq.com

Received 19 October 2020; Accepted 05 January 2021; Published 25 March 2021

Abstract

Photosynthetic characteristics and expression patterns of the photosynthesis-related genes in the high-yield mulberry variety E'Sang 1 (E1) and normal mulberry variety Husang 32 (H32) were investigated in this study. The observation of daily variation of photosynthesis in E1 and H32 indicated that the peak of net photosynthetic rate (P_n) in E1 variety was significantly higher than that in H32 ($P < 0.05$). Meanwhile, the P_n -PAR and P_n -Ci responses of E1 and H32 were evaluated, and the results showed that the carboxylation efficiency and compensation saturation point were much higher in E1 rather than H32. Importantly, the photosystem II actual photochemical efficiency and photochemical quenching coefficient in the leaves of E1 were significantly higher than those in H32 ($P < 0.05$). Also, the activity of RuBP in E1 was higher than that in H32 ($P > 0.05$). Based on the RNA-seq data, a total of 3,356 differentially expressed genes (DEGs) were detected among different time points between E1 and H32. Of these, 1,136 DEGs were involved in the metabolic pathways, including three main photosynthesis-related metabolic pathways (*i.e.*, carbon fixation in photosynthetic organisms, carbon metabolism, and porphyrin and chlorophyll metabolism). Meanwhile, 10 novel DEGs related to photosynthesis were detected, and four potential key genes of them could account for the differences in net photosynthetic rate and yield between H32 and E1. This study could provide important insights into the molecular breeding of mulberry varieties with high photosynthetic efficiency and contribute to understanding the genetic mechanism of photosynthesis. © 2021 Friends Science Publishers

Keywords: Mulberry; Photosynthetic characteristics; Chlorophyll fluorescence characteristics; Gene expression

Introduction

Photosynthesis in higher plants is an extremely complex process enabling material production (Wu *et al.* 2017; Feng *et al.* 2019). The photosynthesis characteristics of plants have been a hot topic for many years and the genetic mechanisms of better light use efficiency of a plant are important for underlying the photosynthesis characteristics (Shen *et al.* 2008; Ryu *et al.* 2019). *Morus alba* L. is a deciduous tree or shrub. As a traditional feed for silkworm (*Bombyx mori* L.), mulberry leaves are important materials in the sericulture industry and have great nutritional and medicinal value. Currently, mulberry leaves and mulberries are listed by the Ministry of Health of China as “one of the agricultural products that are both food and medicine”. Besides, mulberries have spread throughout the world and are highly praised for their unique flavor and impressive composition of nutrients.

Previously, most photosynthesis studies in mulberry trees mainly focused on the effects of stress and artificial cultivation techniques on their photosynthetic characteristics

(Tezara *et al.* 1999; Peng *et al.* 2015; Nemali and Iersel 2019). To our knowledge, little information on photosynthetic characteristics among different mulberry varieties is available. Some studies focused on the effects of abiotic stresses on photosynthesis of mulberry. For instance, Ramanjulu *et al.* (1998) compared the effects of water stress on photosynthesis of the drought tolerant and sensitive mulberry cultivars and found that some photosynthetic characters were different between two different cultivars. Also, the effects of salinity, waterlogging and thermal stresses on photosynthesis of mulberry varieties were also investigated in previous studies (Agastian *et al.* 2000; Chaitanya *et al.* 2003; Yu *et al.* 2013). To investigate the biological regulation mechanisms of the difference of photosynthesis and yield between two different mulberry varieties under natural growth conditions, the major physiological differences in photosynthesis were compared between the high-yield mulberry variety E'Sang 1 (E1) and normal mulberry variety Husang 32 (H32) (Li *et al.* 2014). These two varieties have been widely planted in Yangtze river basin of China for many years. Of these, H32 was bred

in 1978 and E1 is a newly bred variety which has better performance of stress tolerance and yield (Ye *et al.* 2010). Meanwhile, RNA-seq of leaves in different stages of these two mulberry varieties was conducted to identify the potential key genes related to photosynthesis. Although many RNA-seq studies related to mulberry have been reported (Dai *et al.* 2015; Wang *et al.* 2018; Dai *et al.* 2020), the genetic dynamics of photosynthesis related genes in mulberry were still rarely studied. This study aimed to address two main questions, (1) the physiological difference of photosynthesis in the mulberry varieties and (2) unveiling the gene regulation difference of photosynthesis in the mulberry varieties. This study contributes to underlying the biological mechanism of photosynthetic characteristics between the two different mulberry varieties under natural conditions.

Materials and Methods

Sampling

Two mulberry varieties E'Sang1 (E1) and Husang 32 (H32) were cultivated to form middle trunks and planted in 1996 at a density of 133 × 67 cm in the Mulberry Germplasm Resource Garden in Hubei Province of China. Test plots with ground leveling and uniform land fertility were selected. Experiments were conducted in triplicate. Three mulberry trees with similar trunk girth, crown diameter, and tree vigor were selected from a test plot for sampling. Pruning was conducted in summer (July and August). Prevention and treatment of mulberry pests and shoot thinning were conducted to ensure a good group structure for leaf production. The soil in the test field was typical yellow-brown soil with moderate fertility and slight acidity. The pH values ranged from 5.6 to 6.5, and the organic matter contents were above average. The sampling was performed from 2014 to 2019.

Measurement of photosynthetic characters

The net photosynthetic rate (P_n), stomatal conductance (G_s), C_i , and transpiration rate (Tr) of mulberry leaves were determined using an LI-6400XT portable photosynthesis analyzer manufactured by LI-COR (Lincoln, NE, USA) (Chen *et al.* 2010). Daily variation in photosynthesis was measured. The leaves were selected from three well-illuminated top shoots of mulberry trees. One leaf with normal function was selected from each shoot (from leaf positions 5–7). The measurement period was from 6:00 to 18:00. Measurements were performed once every 2 h, with three replicates; The P_n -photosynthetically active radiation (PAR) and P_n - C_i response curves were also evaluated. For P_n -PAR response curves, 14 gradients from 0 to 1,800 $\mu\text{mol}/(\text{m}^2\cdot\text{s})$ were set, and the atmospheric CO_2 concentration was 400 $\mu\text{mol}/\text{mol}$. The initial slope of the P_n -PAR response curve $dP_n/dPAR$ was obtained by linear regression (0–200 $\mu\text{mol}/(\text{m}^2\cdot\text{s})$), which showed the apparent

quantum efficiency (AQY). The light compensation point (LCP) and light saturation point (LSP) were calculated using a fitting curve equation ($y=ax^2+bx+c$) (Peñuelas *et al.* 1998). The P_n - C_i response curves were measured in the same period. Twelve concentrations (0–1500 $\mu\text{mol}/\text{mol}$) were used for CO_2 and PAR was 1200 $\mu\text{mol}/(\text{m}^2\cdot\text{s})$. The initial slope dP_n/dC_i of the P_n - C_i response curve was obtained by linear regression (0–200 $\mu\text{mol}/\text{mol}$), which was the carboxylation efficiency (CE). The CO_2 compensation point (CCP) and saturation point (CSP) were calculated using the P_n - C_i response curve equation (Zhou *et al.* 2019).

Chlorophyll fluorescence measurement

Chlorophyll fluorescence was determined using a fluorescent leaf chamber of the LI-6400 photosynthesis analyzer. Leaf positions and leaves were selected as described above. Firstly, the leaves were completely wrapped with aluminum foil for 12–24 h of shading before the experiment. When mulberry leaves were completely dark-adapted, they were accurately measured from 5:30 to 7:00 in the morning. Each sample was measured 6 times.

During the measurement, the detection light was turned on to determine the minimum initial fluorescence (F_0), and all PSII reaction centers were open. After the F_0 was measured, the de-excitation of leaves was achieved using intense saturated pulsed light, and dark-adapted maximum fluorescence (F_m) was measured. Subsequently, the leaves were exposed to continuous photochemically active light [PPFD=1200 $\mu\text{mol}/(\text{m}^2\cdot\text{s})$] for 30 min to determine the steady-state fluorescence (F_s). The action light was turned on to provide continuous and appropriate supersaturated light (PPFD=2000 $\mu\text{mol}/(\text{m}^2\cdot\text{s})$) to illuminate the leaves, and the maximum fluorescence (F_m') after light adaptation was obtained. After the measurement, the action and detection lights were turned off and far-red light was applied to measure the light-adapted initial fluorescence (F_0'). Other chlorophyll fluorescence parameters such as photosystem II (PSII) maximum photochemical efficiency (F_v/F_m), PSII actual photochemical efficiency (ΦPSII), photochemical quenching coefficient (qP), non-photochemical quenching (NPQ), and PSII electron transfer rate (ETR) were automatically calculated, and the main chlorophyll fluorescence parameters were calculated as follows:

- (1) PSII maximum quantum efficiency: $F_v/F_m=(F_m - F_0)/F_m$ (Genty *et al.* 1989)
- (2) PSII actual quantum efficiency: $\Phi\text{PSII}=\Delta F/F_m'=(F_m' - F_s)/F_m'$ (Genty *et al.* 1989)
- (3) Apparent electron transfer rate: $\text{ETR}=0.5\times 0.84\times\Phi\text{PSII}\times\text{PPFD}$ (Demmig *et al.* 1987)
- (4) Photochemical quenching coefficient: $qP=(F_m' - F_s)/(F_m' - F_0')$
- (5) Non-photochemical quenching: $\text{NPQ}=(F_m - F_m')/F_m'$

Measurement of physiological and biochemical characters

Chlorophyll was extracted using phosphate-buffer containing 80% acetone and analyzed at 646.6 nm, 663.6 nm and 750 nm, respectively (Porra *et al.* 1989; Brouwer *et al.* 2012) using a Spectrophotometer. Rubisco activity was measured by conducting coupled spectrophotometric assays (Kubien *et al.* 2011).

Statistical analysis

Mean values of five values were calculated using Microsoft Office Excel 2007. The ANOVA (analysis of variance) was performed with SPSS software (SPSS, IL, USA).

RNA-seq of two mulberry varieties

RNA extraction and RNA-seq: Leaf samples of two mulberry varieties were collected at the time of peak and trough of the daily variation curve of photosynthesis and frozen in liquid nitrogen. A total of 12 leaf samples were prepared, and they included 2 time points (10:00 and 12:00) of the two mulberry varieties; each time point has three biological replicates. The RNA of leaf samples was extracted using TRIzol reagent (Invitrogen, Thermo Fisher Scientific, USA) following the instruction. The quality of RNA sample was accessed with NanoDrop 2000 and Agilent 2100. After quality control, the qualified RNA was used for construction of Illumina RNA-seq libraries with Illumina TruSeq sample Prep Kit. The sequencing was performed with Illumina HiSeq Xten (San Diego, CA, USA) with 150 paired ends.

RNA-seq data mining

The raw reads generated from Illumina system were filtered and trimmed with fast QC and fastp. Subsequently, the obtained clean reads were mapped to the mulberry genome (NCBI genome accession number: 17692) with TopHat2. The FPKM values of gene were calculated using Cufflinks. The novel genes identified in this study were annotated with the public databases, including NCBI NR database, Swiss-Prot, GO, KOG, Pfam, and KEGG.

The samples collected at two time points for E1 and H32 varieties were named as E1-10, E1-12, H32-10 and H32-12, respectively. A criterion of fold-change ≥ 2 and false discovery rate (FDR) < 0.01 was used to detect the differentially expressed genes (DEGs). The photosynthesis-related DEGs were screened out from the two mulberry varieties with different yields. GO and KEGG pathway enrichment analyses of DEGs were performed with DAVID 6.7 tools.

Validation of expression levels of DEGS

The first-strand cDNA was synthesized using oligo-dT

(TaKaRa, Shiga, Japan). RT-qPCR was performed using Light Cycler 480 (Roche, Basel, Switzerland) in 20 μL based on iTaq SYBR Green Mix (TakaRa, Shiga, Japan). The reaction conditions were 95°C for 3 min, followed by 40 cycles of 94°C for 10 s, 55°C for 10 s, and 72°C for 30 s. The expression levels were calculated relative to the expression levels of β -actin and *GADPH* by using the $2^{-\Delta\Delta\text{Ct}}$ method (Livak and Schmittgen 2001). Primers were designed using NCBI primer design program. The sequences of primers are shown in Table S1.

Results

Daily variation of photosynthesis of two mulberry varieties

The photosynthetic rate (P_n) of the two mulberry varieties from 6:00 to 18:00 showed a typical bimodal curve (Fig. 1A). The first peak appeared at 10:00, while the second peak appeared at 14:00. The P_n peaks of the leaves from E1 and H32 were 34.56 and 32.65 $\mu\text{mol}/(\text{m}^2\cdot\text{s})$, respectively. Notably, the peak P_n of E1 was significantly higher than that of H32 ($P < 0.05$). The G_s and C_i were gradually decreasing from 6:00 to 18:00 (Fig. 1B-C). The curve of transpiration rate (T_r) (transport resistance of CO_2 and water) values was unimodal (Fig. 1D), which was increasing at 6:00 and reached a peak at 12:00 then gradually decreased. The T_r peaks of E1 and H32 leaves were 6.30 and 10.56 $\text{mmol}/(\text{m}^2\cdot\text{s})$, respectively. The peak of T_r in H32 was significantly higher than that in E1 ($P < 0.05$).

P_n -PAR and P_n - C_i response of the E1 and H32 varieties

We found that carboxylation efficiency (CE) and CO_2 saturation point (CSP) were higher in E1 rather than H32, while AQY, LCP, LSP, and CCP were higher in H32. The detailed summary is shown in Table 1. The LSP values of leaves in H32 and E1 were 1500 and 1400 $\mu\text{mol}/(\text{m}^2\cdot\text{s})$, respectively, and the LCP values were 47.930 and 31.182 $\mu\text{mol}/(\text{m}^2\cdot\text{s})$, respectively, which indicated that the ability of accumulating photosynthate under weak light in E1 was stronger than that in H32. The CCP values of H32 and E1 were 74.618 and 68.724 $\mu\text{mol}/\text{mol}$, respectively, indicating that E1 has higher utilization efficiency of low CO_2 concentration. The CSP values in E1 and H32 were 1212.5 and 1162.5 $\mu\text{mol}/\text{mol}$, respectively, implying that the CO_2 concentration range utilized by E1 was greater than that of H32 (Cannell and Thornley 1998).

Chlorophyll fluorescence parameters in E1 and H32 varieties

As shown in Fig. 2A and Fig. 2B, no significant difference was observed in the F_o and F_m between the two mulberry varieties ($P > 0.05$) as well as the initial fluorescence between E1 and H32 (Fig. 2C). The ΦPSII and q_P were

Table 1: Comparison of major photosynthetic physiological parameters of the two mulberry varieties

Variety	AQY/($\mu\text{mol}\cdot\mu\text{mol}^{-1}$)	LCP/($\mu\text{mol}\cdot\text{m}^{-2}\cdot\text{s}^{-1}$)	LSP/($\mu\text{mol}\cdot\text{m}^{-2}\cdot\text{s}^{-1}$)	CE/($\text{mol}\cdot\text{m}^{-2}\cdot\text{s}^{-1}$)	CCP/($\mu\text{mol}\cdot\text{mol}^{-1}$)	CSP/($\mu\text{mol}\cdot\text{mol}^{-1}$)
H32	0.057	47.930	1500	0.055	74.618	1162.500
E1	0.055	31.182	1400	0.058	68.724	1212.500

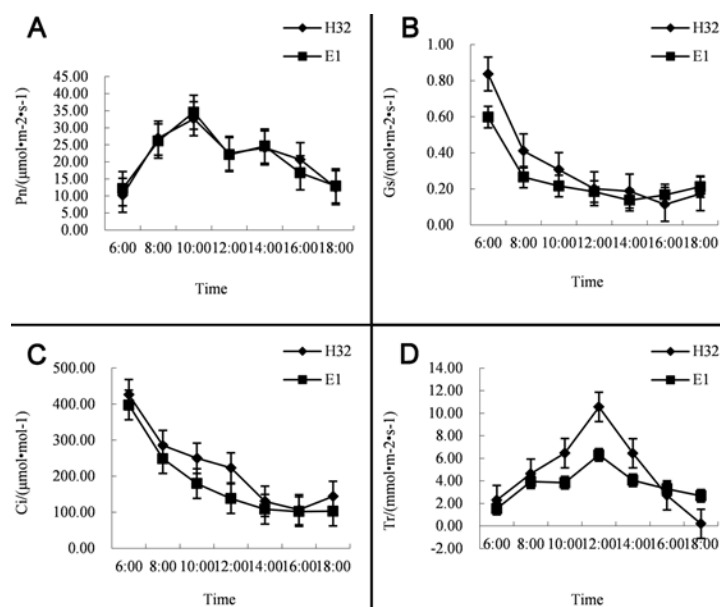


Fig. 1: Daily variation in gas exchange parameters of mulberry leaves. (A) Pn represents photosynthetic rate; (B) Gs represents stomatal conductance; (C) Ci represents intercellular CO_2 concentration; (D) Tr represents transpiration rate; Error bars represent standard error. Different letters on error bars indicate significant differences at $P < 0.01$. Symbols are the same in the Figs

greater in the leaves of E1 than in H32 ($P < 0.05$) (Fig. 2D-E), and the NPQ and ETR differed between the two different mulberry varieties. ΦPSII and qP in the leaves of H32 were greater than those in E1 ($P < 0.05$) (Fig. 2F-G).

Chlorophyll content and activity of RuBP carboxylase

After determining the photosynthesis and chlorophyll fluorescence parameters, leaf samples were collected to determine chlorophyll content and RuBP activity. We found that the contents of chlorophyll a, chlorophyll b, and total chlorophyll in H32 were significantly lower than those in E1 ($P < 0.05$) (Fig. 3A-B), which showed that the level of photosynthesis in E1 was much higher than in H32. Meanwhile, the RuBP activities in E1 and H32 were similar ($P > 0.05$).

Gene expression profiling of the two different mulberry varieties

Identification of differentially expressed genes (DEGs):

A total of 23,136,096 and 27,147,665 clean reads were obtained for the two libraries (H32-10 and H32-12), respectively, in H32 variety. The numbers of clean reads obtained for two E1 libraries (E1-10 and E1-12) were 27,641,855 and 30,242,866, respectively. The clean reads were mapped to the reference genome, and the distribution

of read coverage on the genome is shown in Fig. S1. The numbers of DEGs identified from the pairwise comparisons are shown in Fig. 4 and the 3,359 DEGs is listed in Table S1. A total of 507 DEGs between H32-10 and H32-12, and 297 DEGs were significantly up-regulated. Likewise, 585 DEGs were detected between E1-10 and E1-12, and 339 potential key genes were up-regulated. To investigate the difference of gene expression between two varieties, the comparison was also performed with H32-10 vs. E1-10. A total of 1,179 DEGs were detected between H32-10 and E1-10, including 781 up-regulated genes and 398 down-regulated genes. Furthermore, 1,085 DEGs (612 up-regulated and 473 down-regulated genes) were detected in the comparison of H32-12 vs. E1-12.

Functional analysis of DEGs

The GO annotation of DEGs is shown in Fig. S2. The results of GO enrichment analyses showed that the DEGs were significantly enriched in some important GO terms, including branched-chain amino acid biosynthetic process, chalcone biosynthetic process, regulation of anthocyanin biosynthetic process, pectin catabolic process, organelle assembly, drug transmembrane transport, cellular biogenic amine biosynthetic process, defense response signaling pathway, resistance gene-dependent, and glycine catabolic process.

Table 2: Photosynthesis-related metabolic pathways with significantly enriched DEGs

Comparison	KO ID	Pathway	Number of DEGs
H32-10 vs. H32-12	ko00710	Carbon fixation in photosynthetic organisms	5
	ko01200	Carbon metabolism	7
	ko00860	Porphyrin and chlorophyll metabolism	4
E1-10 vs. E1-12	ko00710	Carbon fixation in photosynthetic organisms	4
	ko01200	Carbon metabolism	6
	ko00860	Porphyrin and chlorophyll metabolism	2
H32-10 vs. E1-10	ko00710	Carbon fixation in photosynthetic organisms	4
	ko01200	Carbon metabolism	9
	ko00860	Porphyrin and chlorophyll metabolism	0
H32-12 vs. E1-12	ko00710	Carbon fixation in photosynthetic organisms	2
	ko01200	Carbon metabolism	4
	ko00860	Porphyrin and chlorophyll metabolism	0

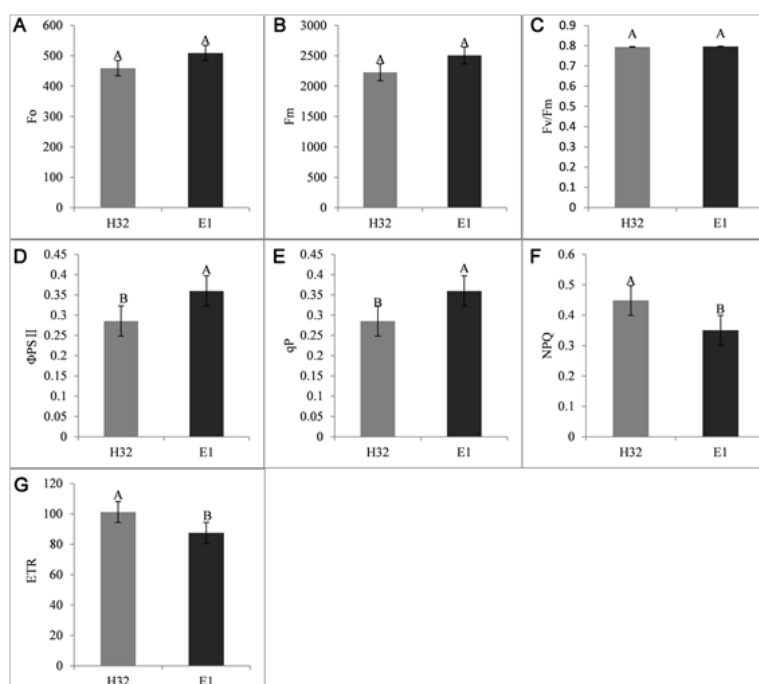


Fig. 2: Chlorophyll fluorescence parameters of mulberry leaves. (A) F_o represents minimum fluorescence. (B) F_m represents maximum fluorescence. (C) F_v/F_m represents the ratio of variable to maximal chlorophyll fluorescence. (D) Φ_{PSII} represents actual photochemical quantum yield. (E) q_P represents photochemical quenching. (F) NPQ represents amount of light energy. (G) ETR represents electron transport rate. Error bars represent standard error. Different letters on error bars indicate significant differences at $P < 0.01$

To deeply explore the key genes and potential pathway involved in photosynthesis, the DEGs were classified into KEGG pathway, and the metabolic pathway was selected to focus on. The summary of DEGs related to metabolic pathway is shown in Fig. S3. In detail, a total of 232, 190, 380 and 334 DEGs were involved in metabolic pathways in H32-10 vs. H32-12, E1-10 vs. E1-12, H32-10 vs. E1-10, and H32-12 vs. E1-12, respectively. More importantly, the DEGs related to three photosynthesis-related metabolic pathways, *i.e.*, carbon fixation in photosynthetic organisms, carbon metabolism, porphyrin and chlorophyll metabolism, were summarized (Table 2). The expression levels of photosynthesis-related genes in metabolic pathways are shown in Table 3. The LOC4331897 (1,4-dihydroxy-2-naphthoate polyprenyltransferase), which is involved in

carbon fixation in photosynthetic organisms, was significantly up-regulated in E1-12 compared with E1-10, but interestingly, it was not up-regulated in H32-10 vs. H32-12. As a key factor in porphyrin and chlorophyll metabolism, the transcripts of chlorophyllase were down-regulated in E1-10 vs. E1-12, but they were not differentially expressed in H32-10 vs. H32-12. Meanwhile, some transcripts of genes participating in carbon fixation were differentially expressed between H32 and E1 varieties. For instance, the transcripts of pyruvate phosphate dikinase were down-regulated and NADP-dependent malic enzyme was up-regulated in H32-12 vs. E1-12. Moreover, the similar dynamics of these genes were observed in the H32-10 vs. E1-10. As an important gene in the porphyrin and chlorophyll metabolism, the transcripts of chlorophyllase-1 were up-regulated in H32-12

Table 3: Summary of photosynthesis-related genes in the metabolic pathways

Comparison	Biological process	KO ID	Gene	Up/Down	FDR	Log2FC		
E1-10 vs. E1-12	carbon fixation in photosynthetic organisms	ko00710	Phosphoenol pyruvate carboxylase 2	Down	1.01E-21	-1.07455		
		K02548	1,4-dihydroxy-2-naphthoate polyprenyltransferase	Up	2.58E-13	1.154945		
	carbon metabolism	ko00710	Fructose-bisphosphate aldolase 1	Down	4.83E-12	-1.18374		
		ko00710	Fructose-bisphosphate aldolase 2	Down	3.19E-27	-1.5095		
		ko00710	Fructose-1,6-bisphosphatase	Down	5.89E-20	-1.00595		
		ko01200	Phosphoenolpyruvate carboxylase 2	Down	1.01E-21	-1.07455		
		ko01200	Fructose-bisphosphate aldolase 1	Down	4.83E-12	-1.18374		
		ko01200	Fructose-bisphosphate aldolase 2	Down	3.19E-27	-1.5095		
		ko01200	Fructose-1,6-bisphosphatase	Down	5.89E-20	-1.00595		
		ko01200	D-3-phosphoglycerate dehydrogenase	Down	3.47E-23	-1.09837		
		ko01200	glucose-6-phosphate 1-dehydrogenase	Up	3.76E-30	1.452002		
		K02548	1,4-dihydroxy-2-naphthoate polyprenyltransferase	Up	2.58E-13	1.154945		
	porphyrin and chlorophyll metabolism	ko00860	Chlorophyllase	Down	0.000149	-1.96728		
		ko00860	Chlorophyllase-1	Up	1.51E-18	2.689146		
		ko00860	Chlorophyllase-2	Up	4.38E-11	1.741928		
		ko00860	Protochlorophyllide reductase	Up	2.42E-25	1.722631		
	H32-10 vs. H32-12	carbon fixation in photosynthetic organisms	ko00710	Fructose-bisphosphate aldolase 1	Down	1.60E-06	-1.18952	
			ko00710	Fructose-bisphosphate aldolase 2	Down	3.19E-27	-1.5095	
			ko00710	Transketolase	Down	0.00013	-1.00502	
		carbon metabolism	ko00710	Fructose-1,6-bisphosphatase	Down	0.000597	-1.15076	
ko01200			Fructose-bisphosphate aldolase, cytoplasmic isozyme 1	Down	1.60E-12	-1.18952		
ko01200			putative fructose-bisphosphate aldolase 2	Down	9.29E-10	-1.27176		
ko01200			Fructose-1,6-bisphosphatase	Down	0.000597	-1.15076		
porphyrin and chlorophyll metabolism		ko01200	D-3-phosphoglycerate dehydrogenase	Down	7.94E-09	-1.11896		
		ko01200	glucose-6-phosphate 1-dehydrogenase, chloroplastic-like	Up	1.47E-23	1.790828		
		ko01200	Transketolase	Down	0.00013	-1.00502		
		ko00860	Chlorophyllase-1	Up	7.25E-05	1.28331		
		ko00860	Protochlorophyllide reductase	Up	6.95E-24	1.837399		
		H32-12 vs. E1-12	carbon fixation in photosynthetic organisms	ko00710	Pyruvate phosphate dikinase	Down	1.31E-29	-1.37241
				ko00710	NADP-dependent malic enzyme	Up	5.70E-11	1.123941
			carbon metabolism	ko01200	D-3-phosphoglycerate dehydrogenase	Down	6.67E-06	-1.775
		ko01200		NADP-dependent malic enzyme	Up	5.70E-11	1.123941	
ko01200	Pyruvate phosphate dikinase	Down		1.31E-29	-1.37241			
ko01200	hypothetical protein L484_016723	Up		1.04E-10				
porphyrin and chlorophyll metabolism	ko00860	Chlorophyllase-1	Up	2.28E-06	-2.37285			
	H32-10 vs. E1-10	carbon fixation in photosynthetic organisms	ko00710	Pyruvate phosphate dikinase	Down	0.000126	-1.06521	
ko00710			Photosystem Q(B) protein	Down	0.004188	-1.04555		
ko00710			NADP-dependent malic enzyme	Up	1.16E-07	1.072298		
carbon metabolism		ko00710	Phosphoenolpyruvate carboxylase, housekeeping isozyme	Up	1.23E-09	1.119376		
		ko01200	hypothetical protein L484_016723	Up	7.31E-08	6.315284		
		ko01200	GRAS domain family, Scarecrow-like protein	Up	0.003807	1.715487		
		ko01200	Pyruvate, phosphate dikinase	Down	0.000126	-1.06521		
		ko01200	Alcohol dehydrogenase-like 2	Up	0.007645	1.411398		
		ko01200	2-oxoglutarate dehydrogenase	Up	3.84E-10	1.150373		
		ko01200	NADP-dependent malic enzyme	Up	1.16E-07	1.072298		
porphyrin and chlorophyll metabolism	ko01200	Phosphoenolpyruvate carboxylase, housekeeping isozyme	Up	1.23E-09	1.119376			
	ko01200	Pyruvate kinase isozyme G	Up	2.30E-07	1.330851			

vs. E1-12, whereas they were not detected in H32-10 vs. E1-10.

Screening of novel photosynthesis-related genes

We compared the transcripts to the reference genome identified the genes which had not been annotated in the genome, the genes with length > 150 bp and more than one exon were remained. According to the functional annotation of 3,359 DEGs, 10 novel DEGs related to photosynthesis were screened out. Of these, 3 genes were down-regulated in H32-10 vs. H32-12 and E1-10 vs. E1-12. Also, 2 up-regulated genes were found in H32-10 vs. E1-10 and H32-12

vs. E1-12. The details of 10 novel genes are shown in Table 4. Five novel genes were differentially expressed in H32-10 vs. H32-12 and E1-10 vs. E1-12, and 3 of them, annotated into carbohydrate transport and metabolism, defense mechanisms, metabolites biosynthesis, and transport and catabolism, were down-regulated in H32-10 and E1-10, while genes (*i.e.*, glucose-6-phosphate 1-dehydrogenase, CHUP1, and chloroplastic) were up-regulated. In the comparisons of E1 and H32 varieties, the novel genes annotated into GTP diphosphokinase RSH3, chloroplastic, translocase of chloroplast 34, chloroplastic, and cytochrome P450 71A2 were down-regulated in H32. These novel genes may play important roles in the net photosynthetic rates between E1

Table 4: Dynamics of candidate genes related to photosynthesis at H32-10 vs. H32-12 and E1-10 vs. E1-12

Gene ID	KOG class	Gene name	Up/Down	FDR	Log2FC
novel_Gene_2229	Carbohydrate transport and metabolism; Amino acid transport and metabolism	Glucose-6-phosphate/phosphate translocator 2, chloroplastic (Precursor) GN=GPT2	Down	5.97E-13	-1.66243
novel_Gene_2532	Defense mechanisms	Phosphoglucan phosphatase LSF2, chloroplastic (Precursor) GN=LSF2	Down	1.76E-21	-1.11158
novel_Gene_2607	Carbohydrate transport and metabolism	Glucose-6-phosphate 1-dehydrogenase, chloroplastic (Precursor)	Up	3.76E-30	1.452002
novel_Gene_3423	Secondary metabolites biosynthesis, transport and catabolism	Cytochrome P450 71D11 (Fragment) GN=CYP71D11	Down	2.17E-16	-1.75873
novel_Gene_3646		Protein CHUP1, chloroplastic GN=CHUP1	Up	1.15E-22	2.259859
Novel_Gene_1405	Signal transduction mechanisms	Probable GTP diphosphokinase RSH3, chloroplastic (Precursor) GN=RSH3	Down	7.07E-08	-3.78629
Novel_Gene_1982		Translocase of chloroplast 34, chloroplastic GN=MUG13.14	Down	7.45E-05	-2.66407
Novel_Gene_2419	Secondary metabolites biosynthesis, transport and catabolism	Cytochrome P450 71A1 GN=CYP71A1	Up	2.85E-10	6.882457
Novel_Gene_2424	Secondary metabolites biosynthesis, transport and catabolism	Cytochrome P450 71A2 GN=CYP71A2	Down	2.99E-23	-1.81672
Novel_Gene_320	Secondary metabolites biosynthesis, transport and catabolism	Cytochrome P450 71D10 GN=CYP71D10	Up	2.16E-20	3.42803

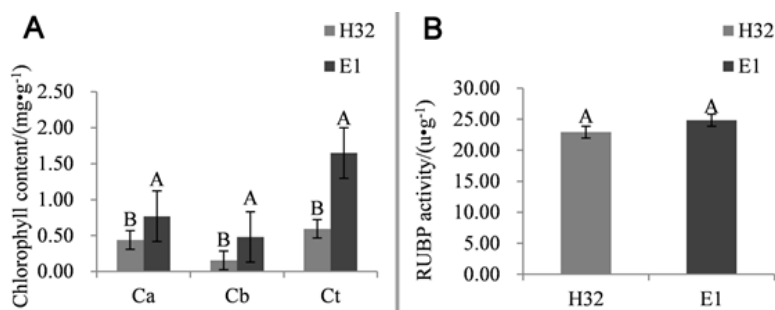


Fig. 3: Comparison of chlorophyll content and RUBP activity in mulberry leaves. (A) Ca represents leaf chlorophyll a content, Cb represents leaf chlorophyll b content, Ct represents leaf total chlorophyll content. (B) RUBP activity represents Ribulose 1,5-bisphosphate carboxylase activity. Error bars represent standard error. Different letters on error bars indicate significant differences at $P < 0.01$

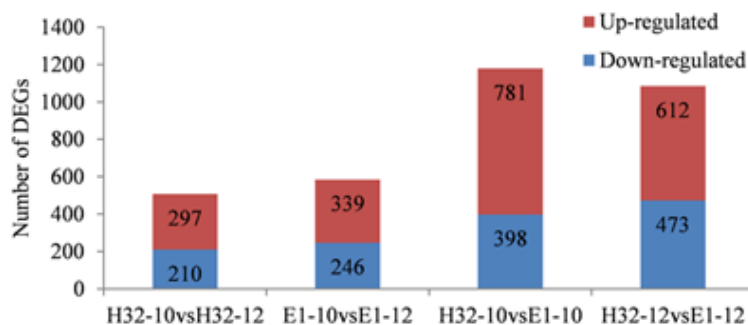


Fig. 4: Statistics of differentially expressed genes in the pairwise comparisons

and H32 at different and the same time intervals.

Validation of RNA-seq data

The expression levels of the 10 novel genes were investigated using RT-qPCR method (Table S2). Five of them (Fig. 5A–E) except Novel_gene_3423 showed significant difference between the time points ($P < 0.05$), and the other five novel genes (Fig. 5F–J) were differentially expressed between the varieties ($P < 0.05$), which coincides with the RNA-seq data. It indicated that the gene expression levels determined by RNA-seq data were reliable in this study.

Discussion

Mulberry is an economic food crop for the domesticated silkworm more than 5000 years (Rudramuni *et al.* 2019). The mulberry varieties (E1 and H32) are two representative varieties which have been widely planted in China, especially in Yangtze River basin. In this study, we comprehensively investigated the daily variations of photosynthetic rate from 6:00 to 18:00 in the E1 and H32. The gas exchange parameters showed obvious difference between the two mulberry varieties, and an increased rate of photosynthesis occurred in E1 variety. According to the results of P_n -PAR and P_n -Ci response, it indicated that E1

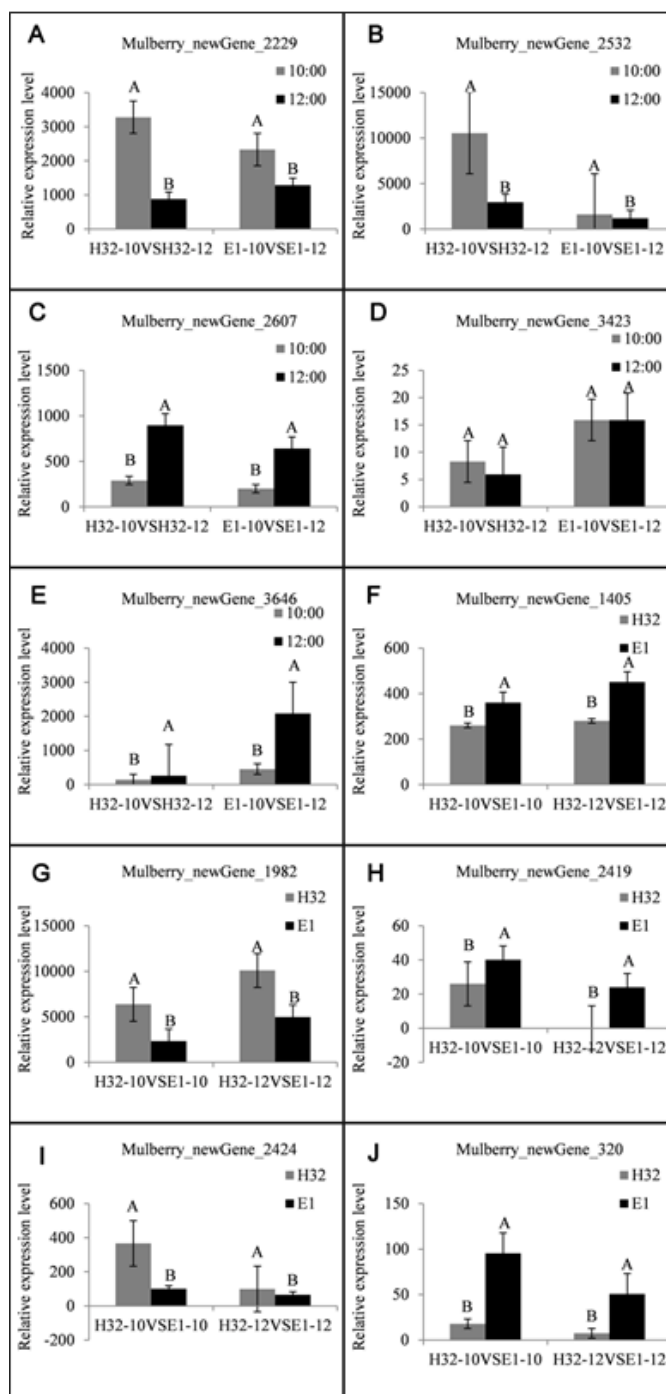


Fig. 5: Quantitative RT-PCR of ten candidate genes related to photosynthesis

had greater photosynthetic capacity than H32 and showed higher potential in accumulating photosynthetic products under weak light intensity. Based on the theory of Farquhar and Sharkey (1982), a higher G_s is a prerequisite for the higher P_n . The enhanced G_s can promote CO_2 movement in the stomatal cavity in response to CO_2 concentration. It has been demonstrated that the primary determinant of crop yield is the cumulative rate of photosynthesis (Lawson *et al.*

2012; Simkin *et al.* 2019), which could account for the difference of yield between two varieties.

Φ_{PSII} is an important indicator of plant photosynthetic capacity and can reflect the proportion of the excitation energy used for the photochemical pathways in the total excitation energy of PSII (Liu *et al.* 2018). qP , a photochemical quenching coefficient, reflects the amount of light energy absorbed by the PSII antenna pigment and used

for the photochemical reaction. In this study, both of Φ PSII and qP in E1 were higher than those in H32, indicating that E1 reflects the increased demand in the Calvin cycle for ATP and NADPH, and an increase in leaves qP indicated an up-regulation of the rate of consumption of reductants and ATP (Lim *et al.* 2020). Meanwhile, the contents of chlorophyll a, chlorophyll b, and chlorophyll in H32 were lower than E1. Overall, most of the estimated values of photosynthetic characters were significantly larger in E1 than in H32, which coincided with the previous study (Deng *et al.* 2012).

Gene regulation plays important roles on photosynthesis in plants, particularly the genes in metabolic pathway mediating the efficiency of photosynthesis. In the previous studies (Ding *et al.* 2013; Ashraf and Harris 2013), some important genes involved in photosynthesis have been identified, such as *Sp1*, *Pepc*, *Rbc L* and *Ppdk*. In this study, a number of DEGs was detected between the two varieties. Of these, the DEGs in metabolic pathway were screened out, and three photosynthesis-related metabolic pathways, including carbon fixation, carbon metabolism, and porphyrin and chlorophyll metabolism were detected. Most importantly, the DEGs related to carbon fixation and metabolism was significantly up-regulated in E1 compared with H32. For instance, the gene *Pepc* (Phosphoenolpyruvate carboxylase), which is essential to the production of carbon skeletons for amino acid biosynthesis in plants (Heyduk *et al.* 2019). PEPC is one of the key proteins of photosynthetic pathway which catalyses the initial fixation of atmospheric CO₂. Bandyopadhyay *et al.* (2007) introduced intact maize *pepc* gene in *indica* rice by biolistic transformation and found that the photosynthesis rate of rice was enhanced in high temperature conditions. Likewise, the up-regulation of NADP-dependent malic enzyme (NADP-ME) in E1 was detected, which catalyzes the oxidative decarboxylation of malate to generate pyruvate, CO₂ and NADPH. In plants, the photosynthetic NADP-MEs supply CO₂ for carbon fixation in the bundle sheath chloroplasts of C4 plants and the cytosol of crassulacean acid metabolism (CAM) plants (Alvarez *et al.* 2019; Chen *et al.* 2019).

Conclusion

In the comparison of E1 and H32, many DEGs related to the porphyrin and chlorophyll metabolism were identified, which is related to the synthesis, utilization and degradation of porphyrin and chlorophyll, a group of green magnesium-containing porphyrin derivatives occurring in photosynthetic plants. Besides, some novel DEGs were identified in this study, which were not annotated in the reference genome. These novel genes were annotated against the public databases, and we found most of them could match the homologue genes in the databases and a few novel genes were involved in photosynthesis of mulberry. These novel genes should be deeply explored in our further study.

Acknowledgement

The study was funded by National Fund for Modern Agricultural Industry Technology System Construction (No: CARS-18-ZJ0208).

Author Contributions

Conceived and designed the experiments: Yong Li, Chuxiong Zhuang and Wen Deng; Performed the experiments: Yong Li, Cui Yu and Rongli Mo; Analysed the data: Yong Li, Chao Xiong and Zhixian Zhu; Contributed reagents/materials/analysis tools: Yong Li and Xingming Hu; Contributed to the writing of the manuscript: Yong Li All of the authors reviewed the manuscript

Conflict of Interest

The authors of this article have no conflict of interest

Data Availability Declaration

The authors declare that data reported in this article are available with the corresponding author and will be produced on demand

References

- Agastian P, S Kingsley, M Vivekanandan (2000). Effect of salinity on photosynthesis and biochemical characteristics in mulberry genotypes. *Photosynthetica* 38:287–290
- Alvarez CE, A Bovdilova, A Höppner, CC Wolff, M Saigo, F Trajtenberg, MJ Lercher (2019). Molecular adaptations of NADP-malic enzyme for its function in C4 photosynthesis in grasses. *Nat Plants* 5:755–765
- Ashraf M, PJ Harris (2013). Photosynthesis under stressful environments: An overview. *Photosynthetica* 51:163–190
- Bandyopadhyay A, K Datta, J Zhang, W Yang, S Raychaudhuri, M Miyao, SK Datta (2007). Enhanced photosynthesis rate in genetically engineered *indica* rice expressing *pepc* gene cloned from maize. *Plant Sci* 172:1204–1209
- Brouwer B, A Ziolkowska, M Bagard, O Keech, P Gardstrom (2012). The impact of light intensity on shade-induced leaf senescence. *Plant Cell Environ* 35:1084–1098
- Cannell MGR, JHM Thornley (1998). Temperature and CO₂ Responses of Leaf and Canopy Photosynthesis: A clarification using the non-rectangular hyperbola model of photosynthesis. *Ann Bot* 82:883–892
- Chaitanya KV, PP Jutur, D Sundar, AR Reddy (2003). Water stress effects on photosynthesis in different mulberry cultivars. *Plant Growth Regul* 40:75–80
- Chen F, L Chen, H Zhao, H Korpelainen, C Li (2010). Sex-specific responses and tolerances of *Populus cathayana* to salinity. *Physiol Plantarum* 140:163–173
- Chen Q, B Wang, H Ding, J Zhang, S Li (2019). The role of NADP-malic enzyme in plants under stress. *Plant Sci* 281:206–212
- Dai F, G Luo, Z Li, X Wei, Z Wang, S Lin, C Tang (2020). Physiological and transcriptomic analyses of mulberry (*Morus atropurpurea*) response to cadmium stress. *Ecotoxicol Environ Saf* 205:111298
- Dai F, Z Wang, G Luo, C Tang (2015). Phenotypic and transcriptomic analyses of autotetraploid and diploid mulberry (*Morus alba* L.). *Intl J Mol Sci* 16:22938–22956
- Demmig B, K Winter, A Kruger, FC Czygan (1987). Photoinhibition and zeaxanthin formation in intact leaves: A possible role of the xanthophyll cycle in the dissipation of excess light energy. *Plant Physiol* 84:218–224

- Deng Y, J Li, S Wu, Y Zhu, Y Chen, F He (2006). Integrated nr database in protein annotation system and its localization. *Comput Eng* 32:71–72
- Ding ZS, SH Huang, BY Zhou, XF Sun, M Zhao (2013). Over-expression of phosphoenolpyruvate carboxylase cDNA from C4 millet (*Seteria italica*) increase rice photosynthesis and yield under upland condition but not in wetland fields. *Plant Biotechnol Rep* 7:155–163
- Farquhar GD, TD Sharkey (1982). Stomatal Conductance and Photosynthesis. *Annu Rev Plant Physiol* 33:317–345
- Feng L, MA Raza, Z Li, Y Chen, MHB Khalid, J Du, Z Zhang (2019). The influence of light intensity and leaf movement on photosynthesis characteristics and carbon balance of soybean. *Front Plant Sci* 9; Article 1952
- Genty B, JM Briantais, NR Baker (1989). The relationship between the quantum yield of photosynthetic electron transport and quenching of chlorophyll fluorescence. *Biochim Biophys Acta* 990:87–92
- Heyduk K, JJ Moreno-Villena, IS Gilman, PA Christin, EJ Edwards (2019). The genetics of convergent evolution: Insights from plant photosynthesis. *Nat Rev Genet* 20:485–493
- Kubien DS, CM Brown, HJ Kane (2011). Quantifying the amount and activity of Rubisco in leaves. *Meth Mol Biol* 684:349–362
- Lawson T, DM Kramer, CA Raines (2012). Improving yield by exploiting mechanisms underlying natural variation of photosynthesis. *Curr Opin Biotechnol* 23:215–220
- Li Y, C Ye, W Deng, YU Cui, X Hu, C Xiong, B Peng, H Shi (2014). Effects of spring-cutting on photosynthetic physiological parameters of *Morus alba* L. cv. E-sang No. 1. *Hubei Agric Sci* 53:4885–4891
- Lim SL, CP Voon, X Guan, Y Yang, P Gardeström, BL Lim (2020). In planta study of photosynthesis and photorespiration using NADPH and NADH/NAD⁺ fluorescent protein sensors. *Nat Commun* 11; Article 3238
- Liu Y, T Wang, S Fang, M Zhou, J Qin (2018). Responses of morphology, gas exchange, photochemical activity of photosystem II, and antioxidant balance in *Cyclocarya paliurus* to light spectra. *Front Plant Sci* 9:1704-1718
- Livak KJ, TD Schmittgen (2001). Analysis of relative gene expression data using real-time quantitative PCR and the 2(-Delta Delta C(T)) Method. *Methods* 25:402–408
- Nemali K, MWV Iersel (2019). Relating whole-plant photosynthesis to physiological acclimations at leaf and cellular scales under drought stress in bedding plants. *J Amer Soc Hortic* 144:201–208
- Peng X, L Teng, X Yan, M Zhao, S Shen (2015). The cold responsive mechanism of the paper mulberry: Decreased photosynthesis capacity and increased starch accumulation. *BMC Genomics* 16; Article 898
- Peñuelas J, I Filella, J Llusà, D Siscart, J Piñol (1998). Comparative field study of spring and summer leaf gas exchange and photobiology of the Mediterranean trees *Quercus ilex* and *Phillyrea latifolia*. *J Exp Bot* 49:229–238
- Porra RJ, WA Thompson, PE Kriedemann (1989). Determination of accurate extinction coefficients and simultaneous equations for assaying chlorophylls a and b extracted with four different solvents: Verification of the concentration of chlorophyll standards by atomic absorption spectroscopy. *Biochim Biophys Acta* 975:384–394
- Ramanjulu S, N Sreenivasulu, C Sudhakar (1998). Effect of Water Stress on Photosynthesis in Two Mulberry Genotypes with Different drought Tolerance. *Photosynthetica* 35:279–283
- Rudramuni K, BK Neelaboina, MN Shivkumar, SR Chowdhury (2019). Scope for Region and Season Specific Mulberry Silkworm (*Bombyx mori* L.) in Temperate Regions of Jammu and Kashmir. *Res J Agric Sci* 10:809–814
- Ryu Y, JA Berry, DD Baldocchi (2019). What is global photosynthesis? History, uncertainties and opportunities. *Remot Sens Environ* 223:95–114
- Shen H, Y Tang, H Muraoka, I Washitani (2008). Characteristics of leaf photosynthesis and simulated individual carbon budget in *Primula nutans* under contrasting light and temperature conditions. *J Plant Res* 121:191–200
- Simkin AJ, PE López-Calcagno, CA Raines (2019). Feeding the world: Improving photosynthetic efficiency for sustainable crop production. *J Exp Bot* 70:1119–1140
- Tezara W, VJ Mitchell, SD Driscoll, DW Lawlor (1999). Water stress inhibits plant photosynthesis by decreasing coupling factor and ATP. *Nature* 401:914–917
- Wang D, L Zhao, D Wang, J Liu, X Yu, Y Wei, Z Ouyang (2018). Transcriptome analysis and identification of key genes involved in 1-deoxyxojirimycin biosynthesis of mulberry (*Morus alba* L.). *Peer J* 6; Article e5443
- Wu Y, W Gong, W Yang (2017). Shade inhibits leaf size by controlling cell proliferation and enlargement in soybean. *Sci Rep* 7:9259-9268
- Ye C, W Deng, W Ye (2010). Study on the cultivation of mulberry variety Ersang No. 1 and its application. *Hubei Agric Sci* 49:109–111
- Yu C, S Huang, X Hu, W Deng, C Xiong, C Ye, B Peng (2013). Changes in photosynthesis, chlorophyll fluorescence, and antioxidant enzymes of mulberry (*Morus* spp.) in response to salinity and high-temperature stress. *Biologia* 68:404–413
- Zhou J, Y Li, C Yu, R Mo Z Zhu, Z Dong, X Hu, W Deng (2019). Effects of photosynthetic characteristics and sugar metabolism of fruit mulberry in different breeding methods. *Hubei Agric Sci* 58:89